JCTC Journal of Chemical Theory and Computation

ARTICLE

pubs.acs.org/JCTC

# The Nature of the Idealized Triple Bonds Between Principal Elements and the $\sigma$ Origins of Trans-Bent Geometries—A Valence Bond Study

Elina Ploshnik,[†] David Danovich,[†] Philippe C. Hiberty,*[,‡] and Sason Shaik*[,†]

[†]Institute of Chemistry and The Lise Meitner-Minerva Center for Computational Quantum Chemistry, The Hebrew University of Jerusalem, Jerusalem 91904, Israel

[‡]Laboratoire de Chimie Physique, UMR CNRS 8000, Université de Paris-Sud, 91405 Orsay Cédex, France

Supporting Information

**ABSTRACT:** We describe herein a valence bond (VB) study of 27 triply bonded molecules of the general type X≡Y, where X and Y are main element atoms/fragments from groups 13−15 in the periodic table. The following conclusions were derived from the computational data: (a) Single $\pi$-bond and double $\pi$-bond energies for the entire set correlate with the "*molecular electronegativity*", which is the sum of the X and Y electronegativites for X≡Y. The correlation with the molecular electronegativity establishes a simple rule of periodicity: $\pi$-bonding strength generally increases from left to right in a period and decreases down a column in the periodic table. (b) The $\sigma$ frame invariably prefers trans bending, while $\pi$-bonding gets destabilized and opposes the trans distortion. In HC≡CH, the $\pi$-bonding destabilization overrides the propensity of the $\sigma$ frame to distort, while in the higher row molecules, the $\sigma$ frame wins out and establishes trans-bent molecules with $2^1/_2$ bonds, in accord with recent experimental evidence based on solid state $^{29}$Si NMR of the Sekiguchi compound. Thus, in the trans-bent molecules "*less bonds pay more*". (c) All of the $\pi$ bonds show significant bonding contributions from the resonance energy due to covalent−ionic mixing. This quantity is shown to correlate linearly with the corresponding "*molecular electronegativity*" and to reflect the mechanism required to satisfy the equilibrium condition for the bond. The $\pi$ bonds for molecules possessing high molecular electronegativity are charge-shift bonds, wherein bonding is dominated by the resonance energy of the covalent and ionic forms, rather than by either form by itself.

## I. INTRODUCTION

By the late 19th century, chemists recognized the diversity that the carbon−carbon multiple bonds bring into organic chemistry, and this recognition has ushered in the structural theories of Kekulé, Couper, and others, which eventually led to the development of an electronic theory of bonding by Lewis.[1] Ever since this successful chapter was opened, attempts have been made to create heavier main group analogs, for example, Si−Si double and triple bonds etc. The first attempts to synthesize compounds containing doubly bonded silicon proved, however, unsuccessful and led instead to cyclic oligomers or polymers containing only single covalent bonds.[2] Such failures have led to the formulation of the "Double Bond Rule", which stated that elements having a principal quantum number greater than 2 ($n > 2$) should not be able to form $\pi_{np\text{-}np}$ bonds among themselves or with other elements.[3] For some years, this rule was consensual in the scientific community.

Theory has provided the rationale for the intrinsic weakness of these $\pi_{np\text{-}np}$ ($n > 2$) bonds. An initial qualitative idea,[4] that the weakness of these bonds was due to weak $np-np$ overlaps ($n > 2$), was soon refuted by Mulliken,[5] who suggested that the rarity of these bonds is due to the larger $\pi$ and $\sigma$ bond strength differences in third and higher periods, leading to predominance of $\sigma$-bonded species. Later, Kutzelnigg[6] has shown that, in fact, the propensity for $\pi$-bonding in second row elements is the exception, because these atoms lack core p orbitals, so that the 2p orbitals remain compact and result in short $\sigma$ bonds. These short bond lengths, in turn, favor the $\pi$-type overlaps, leading to strong $\pi$ bonds with a significant overlap population (bond orders etc). On the other hand, $n$p AOs of higher-row atoms develop a radial node to avoid the repulsion with the core $(n-1)p$ AOs and are hence more diffuse than the $n$s AOs. This generally increases the bond lengths relative to second-row atoms, and while this lengthening does not affect the $\sigma$-type overlaps, it diminishes the $\pi$-type overlaps. Consequently in higher-row elements, $\sigma$ bonds become stronger than $\pi$ bonds, and multiply bonded molecules become rare. Thus, quantum chemistry provides theoretical grounds for the difficulties in making multiple bonds beyond second-row atoms, as formulated in the "Double Bond Rule".

As history shows, the formulation of rules, in fact, intensifies the search for cases that break the very same rules. Indeed, the attempts to probe the limits of the "Double Bond Rule" have generated a missionary search after $\pi$-bonded elements from the third period of the periodic table and onward, and these efforts, which rose sharply in the 1980s, are still going strong and progressing to quintuple and sextuple bonding in transition metals.[7]

Already in the 1960s and 1970s, it became evident that despite the consensual acceptance of the "Rule", transient species containing Si=C and Si=Si double bonds do exist. In 1981, the Rule was finally broken when the isolation of stable compounds containing P=P,[8] Si=C,[9] and Si=Si[10] bonds was announced, which were sterically protected by bulky substituents. This strategy was used to create many more molecules containing

**Received:** December 23, 2010
**Published:** March 02, 2011

**Scheme 1. (a) The Segikuchi Compound and (b) Transition between Two Bonding Motifs in REER′**

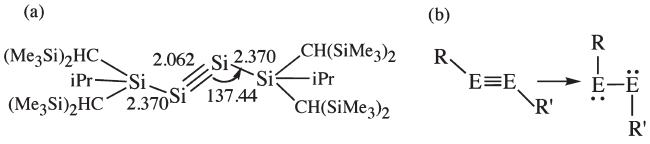


double bonds between heavy main-group elements, and today almost all of the elements in periodic groups 13−16 are a part of the doubly bonded molecular family.[11,12]

The next challenge was making triple bonds, which constitute the focus of the present paper that aims to outline the patterns of the triple bonds in the periodic table of the main elements. Thus, while the research of heavy main-group doubly bonded molecules flourished, analogous triply bonded molecules posed a more difficult challenge. Phosphaalkynes, with a P≡C triple bond, make up one group of compounds that are well-known and characterized[13] and could be made since they do not require extremely large substituents, presumably because the P≡C bond is relatively strong. Thus, HC≡P can be kept for long periods of time at room temperature under reduced pressure,[14] and t-Bu−C≡P is the first stable such molecule.[15] The disulfur cation $S_2I_4^{2+}$, isolated in $S_2I_4(MF_6)_2$ salts (M = As or Sb), was reported to possess a bond order between 2 and 3, according to experimental data and theoretical models.[12] But sulfur and phosphorus are exceptions, and all other heavy main group elements require very bulky substituents in order to create the triple bond.

Let us then follow with a short summary of these experimental efforts in groups 13 and 14:

The molecule OCBBCO, presumably with a B≡B bond, was spotted in reactions of B atoms with CO conducted in solid argon.[15] However, no stable compound of the form $[R-B\equiv B-R]^{-2}$ could be prepared, and the reduction of $RBX_2$ compounds with bulky R ligands has led to insertion products of RB into C−H or C−C bonds.[16] On the other hand, the reduction of $GaCl_2C_6H_3$-2,6-$Trip_2$ with sodium metal produced $Na_2[GaC_6H_3\text{-}2,6\text{-}Trip_2]_2$,[17] but experimental and theoretical[17b,18] evidence showed that the bond order is smaller than three. The geometry around the Ga≡Ga triple bond is trans-bent. No evidence for similar compounds for Al, In, or Tl was reported. Compounds with triple bonds between a group 13 atom and a group 14 or 15 element are restricted to the lightest atoms, like $[R-B\equiv C-R']^-$, which was argued to have partial triple bond character,[19] and R−B≡N,[14] whose triple bond is slightly weaker than the corresponding C≡C bond.

Among the 14 group elements, stable heavier analogs of ethyne became known only recently.[20−23] The first reports appeared in 1999 about the formation of $HC\equiv SiCH_3$, HC≡SiCl, and $H_3CSi\equiv SiCH_3$, but the evidence for these transient species was not conclusive. In 1999, Karni et al. reported[20] the first RC≡SiX (X = F, Cl) molecules, characterized by means of neutralization−reionization (NR) mass spectrometry. Theoretical calculations[20] demonstrated that these RC≡SiX species were detectable, since the barriers for isomerization to the XHC=Si species were too high relative to the energy of the neutral vibrationally excited compound. Initial theoretical ideas for the formation of Si≡Si triple bonds focused mainly on the use of bulky $R_3Si$[21] or the use of bulky aryl groups.[22] In 2004, the first stable compound with a Si≡Si bond (Scheme 1a) was isolated and fully characterized by Sekiguchi et al.,[23] who characterized it as a triple bond based on its structure, UV−vis spectrum, and calculated bond order of 2.6.[24]

It is seen, from Scheme 1a, that the triple bond is protected by very large substituents, larger than the mesitylene groups used by West to protect the doubly bonded Si=Si compound.[10,11] Despite the steric protection, the Si≡Si triple bond in the isolated molecule easily undergoes addition reactions with halogens. As seen from the scheme, the Si≡Si bond length is only slightly shorter than Si=Si (by 3.8%), and like the latter and its heavier analogs with Sn=Sn and Pb=Pb bonds,[25−27] here too the Si≡Si bond is trans-bent. This is obviously in contrast with the linear structure of the acetylenes RC≡CR′ molecules.

In 2001, the formation of germyne, $ArGe\equiv CSiMe_3$, with a triple bond between germanium and carbon, was reported by Bibal et al.,[28] as an intermediate that was trapped by alcohol solvents. This success was followed by a flurry of triply bonded heavier analogs of the Sekiguchi compound. From the structures[29−34] of these R−E≡E−R′ compounds (E = Ge, Sn, and Pb), it became apparent that they undergo a transition between triply and singly bonded motifs, as shown in Scheme 1b. Thus, Power and his co-workers[29] prepared R−E≡E−R′ compounds of E = Si, Ge, Sn, and Pb with formal triple bonds and found that, with the exception of E = Pb, the E−E distances (and REE angles) fell in the range expected for bonds with a bond order between 2 and 3. The molecule with E = Pb, was much more bent (with an RPbPb angle ∼94°) with a bond order of 1, hence resembling more a singly bonded Pb−Pb with lone pairs on the Pb centers (see Scheme 1b). Furthermore, the Sn compound showed sensitivity to the size and nature of R and R′ and, with increased steric bulk around Sn, gave a highly bent (RSnSn angle ∼99°) and singly bonded structure.[29d] These findings confirmed earlier theoretical predictions[32a−c] that the triply and singly bonded forms of REER′ are not too far in energy.

Thus, while all these R−E≡E−R′ compounds are trans-bent like the Sekiguchi compound shown in Scheme 1a, the bending angle is variable, as in Scheme 1b, and this makes the nature of the E−E bonding uncertain and hence vividly debated.[30−34] A recent solid state $^{29}Si$ NMR experimental and theoretical study of the chemical shift tensor and chemical shift anisotropy[35] shows that, despite the bending, the Si≡Si bond in the Segikuchi compound is a "*genuine triple bond composed of a σ-bond and two non-degenerate π-bonds*". Accordingly, our focus on group 14 will be to understand the nature of the E≡E triple bond (E = Si and Ge) and the driving force for its bending, as in the Sekiguchi compound, while refraining from those compounds (E = Sn and Pb) which may undergo a complete transformation to the singly bonded structure (Scheme 1b).

As was mentioned already, phosphoalkynes with C≡P bonds exist.[13] One example of arsaalkynes has been structurally characterized, Mes−C≡As (Mes = mesityl). To the best of our knowledge, no other evidence of stable nitrile analogs has been reported yet, and $N_2$ is the only stable homonuclear molecule with a N≡N triple bond. The corresponding heavier elements' analogues were obtained in the vapor phase. Phosphorus−nitrogen analogues of diazonium salts are also known.[14] Chemists, in fact, keep turning to more candidates,[29e] like the C≡S triply bonded molecule, recently made by Schreiner et al.[36]

All in all, chemistry has by now a considerable family of triply bonded molecules with atoms belonging to third- and fourth-row periods, and this poses a great opportunity to generalize the nature of the triple bond in main elements, with respect to the following two features: The first is the intrinsic strength of the $\pi$ bonds of the triple bond and the variation of this strength with the identity of the atoms that participate in bonding. And the second is the driving force for the distortion from linearity. Our approach is based on VB theory and is a continuation of a preliminary study,[37] which demonstrated that HC≡SiH and HSi≡SiH have 2.5 bonds, and they undergo trans bending since this deformation strongly enhances the $\sigma$ bonding. The same conclusion was recently reached by Landis and Weinhold, based on natural resonance theory (NRT) calculations, leading to bond orders of 2.38−2.79 for HEEH (E = Si, Ge, and Sn).[34] As such, in the first part of the paper, we determine the *intrinsic $\pi$-bond strength* of the linear molecules and compare its dependence on the bonded atoms. Are the *intrinsic $\pi$ bonds* weak? Strong? And how does this quantity vary in the periodic table. Subsequently, we intend to establish the origins of the deviation from linearity: Are these the $\pi$ bonds or the $\sigma$ frame which determine the tendency to distort? And how does this propensity vary with the nature of the "triply-bonded" atom?

The VB method is chosen here because it enables us to achieve these goals with a good measure of lucidity. Thus, in the VB approach, it is possible to achieve a neat separation of the $\sigma$ frame and the $\pi$ bonds in the molecular wave function, so that $\pi$-bond strength and their tendencies can be studied separately from the $\sigma$ frame.[37,38] As much as possible, we shall relate our results to other theoretical interpretation of these issues.

To this end, we selected a sufficiently large stock of 27 triply bonded molecules of the general form $H_nX{\equiv}YH_m$ ($n, m = 0, 1$; X, Y = $B^-$, C, N, $Al^-$, Si, P, $Ga^-$, Ge, and As), which will enable us to draw some generalities. We know that many of these molecules are not linear and that HSiSiH is in fact doubly bridged[7e] and not simply bent. Still, we shall use them as linear ones, in order to establish *the intrinsic bond energies* for one of the two $\pi$ bonds, $D_{\pi}$, as well as for the total $\pi$ system, $D_{2\pi}$, in the triple bonds. Having this stock of data will enable us to draw useful correlations of the intrinsic $\pi$-bonding energy with fundamental properties of the triply bonded atoms. We shall subsequently analyze the driving force for the trans-bending in the third and fourth row molecules as opposed to the linear bond in acetylene, and other second-row molecules. As shall be seen, many of these triply bonded molecule have a strong charge-shift character,[39] and the *total $\pi$-bonding energy correlates well with the sum of the electronegativities of the two bond constituents* rather than with the electronegativity differences.[38a,39b,39c] Furthermore, in line with our previous findings, we shall demonstrate that invariably, within our $\sigma-\pi$ separation, the driving force for bending in the heavier elements[40] is the strengthening of the $\sigma$ bonding, which overcomes the intrinsic tendency of the $\pi$ bonds to maintain a linear geometry, with the strongest possible $\pi$ bonding. Thus, $\pi$ bonding in heavy elements is a story of nonclassical features, when "less bonds pay more",[37] and when bonds may not be classical covalent even if they look like it.

## II. THEORETICAL APPROACHES AND METHODS

**A. A Valence Bond Approach to Intrinsic Bond Energies.** The VB wave function ($\Psi_{VB}$), for a given number of electrons in a given set of atomic orbitals (AOs) or hybrid atomic orbitals (HAOs), is expressed as a linear combination of all of the VB structures ($\Phi_i$) that can be generated by distributing the electrons in the AOs/HAOs so as to form a complete and linearly independent set, as expressed in eq 1:

$$\Psi_{VB} = \sum_i C_i \Phi_i \qquad (1)$$

The set $\{\Phi_i\}$ is referred to as the VB-structure set.[41] For the simplest case, wherein we consider a single $\pi$ bond between the triply bonded X and Y, the VB-structure set consists of one covalent and two ionic structures, as shown in Scheme 2. Note that the covalent structure itself involves a combination of two spin-arrangement patterns ($\alpha\beta$ and $\beta\alpha$), and the resonance between these two structures stabilizes the covalent wave function by the spin-pairing energy, $D_{cov}$.

In the case of two bonds, like the two $\pi$ bonds in triply bonded molecules, we have four electrons that are distributed in four AOs in all possible manners, thereby yielding a VB-structure set with 20 structures. The key ones are shown in Scheme 3, while the rest can be found in the Supporting Information (SI) document (Scheme S1). Two of these VB structures are fully covalent and are shown in Scheme 3, as **1** and **2**. Compound **1** corresponds to the perfectly paired structure, while **2** pairs up the electrons on the fragments. Clearly, **2** is expected to be much less important than **1**. There are also four monoionic structures, **3**−**6**, which are generated from **1** by shifting one electron to the left or right in a single plane, either in *xz* or in *yz*, by analogy to Scheme 2 for a

**Scheme 2. Covalent and Ionic Structures for a $\pi$ Bond and the Two Spin Arrangement Patterns Involved in $\Phi_{cov}$**

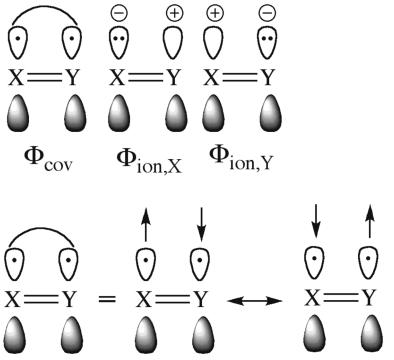


**Scheme 3. Covalent and Monoionic Structures for Two $\pi$ Bonds**

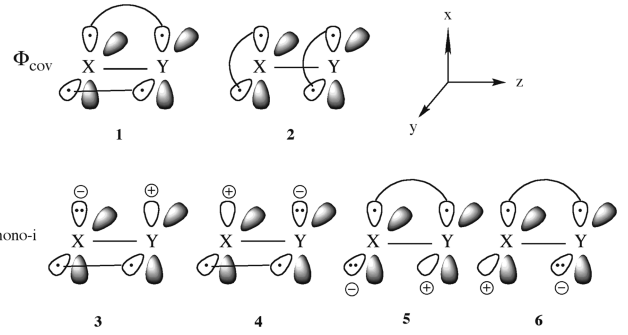

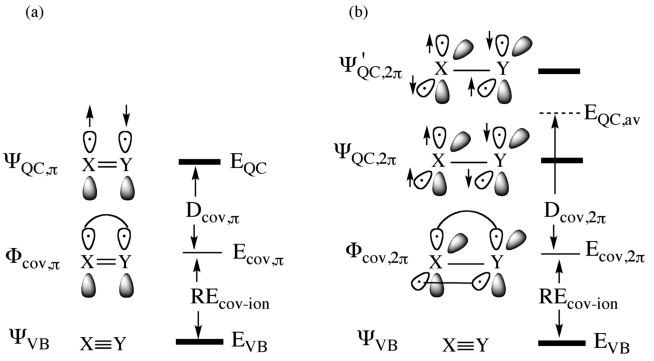


**Figure 1.** Definition of in situ $\pi$-bond energy and its contributing components based on the quasiclassical state (QC) reference (a) for one $\pi$ bond and (b) for $2\pi$ bonds.

single bond. Other conceivable monoionics, which have the positive and negative charges in different planes, e.g., shifting electrons in **2** from $p_x$ to $p_y$, are not used since they are prohibited by symmetry to mix into the wave function. In addition, there are six di-ionic structures that can be generated from the monoionics by shifting the electrons of the covalent bonds either to the left or to the right. These dionics make a very small contribution to the wave function, due to their high energy, and are therefore not shown in Scheme 3. Altogether, the VB wave function of the two $\pi$ bonds is a linear combination of these 12 VB structures.

Generally speaking, whenever the covalent structure has the largest weight, which is the case in all of the molecules studied here, the bonding energy for a single bond or for a double or triple bond is given by the general eq 2:

$$\mathrm{BDE} = \mathrm{BDE_{cov}} + \mathrm{RE_{cov\text{-}ion}} \tag{2}$$

Here, the total bonding energy BDE is a sum of the covalent spin-pairing energy, $\mathrm{BDE_{cov}}$, and the covalent−ionic resonance energy, $\mathrm{RE_{cov\text{-}ion}}$, due to the mixing of the ionic structures into the covalent one(s).[39,41] Both quantities are variational within the corresponding subset of VB structures.

*Determination of the Bonding Energies.* For a single $\sigma$ bond, one can easily determine the thermochemical bonding energy, as a difference between the molecular energy and the energy of the two dissociated radical fragments at infinity. However, for multiply bonded molecules, we cannot dissociate only the $\pi$ bonds, and therefore, the thermochemical $\pi$-bonding energy cannot be determined directly. One could of course dissociate the triple bond into two fragments, e.g., 2HSi for HSi≡SiH, and determine the total bonding energy $\mathrm{BDE}_{2\pi+\sigma}$ for the entire triple bond.[37] However, even then there is no clean way of separating the $\sigma$ and $\pi$ quantities of this $\mathrm{BDE}_{2\pi+\sigma}$ quantity. Additionally, the thermochemical quantity involves considerable energy terms due to reorganization energies of the fragments, which in the example of HSi, involves large demotion energy from the $^4\Sigma^-$ state in the molecule to the $^2\Pi$ state in the fragment.[29d,30,32b,32h,37,40b] Consequently, the $\mathrm{BDE}_{2\pi+\sigma}$ quantity does not reveal the strength of those bonding interactions that are of interest here.

As we have shown amply before,[41,42] these difficulties can be bypassed by defining *a nonbonded reference state*, in which all the $\pi$ bonds are decoupled, and then determine the in situ $\pi$-bond energies as the difference between the energy of the bonded molecule relative to the nonbonded reference energy, $E_{QC}$. This reference nonbonded state is the quasi-classical state, $\Psi_{QC,\pi}$ shown in Figure 1, when a single $\pi$ bond is decoupled as in (a) and $\Psi_{QC,2\pi}$ when two $\pi$ bonds are decoupled as in (b).[37,41,42]

In $\Psi_{QC,n\pi}$ ($n$ = 1, 2) in Figure 1, the electrons of a given $\pi$ bond have only one spin arrangement pattern (only $\alpha\beta$), and therefore this structure by itself has no bonding, which arises only due to the resonance with the second spin arrangement pattern that is required to form a singlet pair (see Scheme 2). As such, the interactions across the $\pi$ bonds in $\Psi_{QC,n\pi}$ involve only classical electron−electron repulsion, nuclear repulsion, and electron−nuclear attraction, and since the fragments are neutral, these terms sum to approximately zero.[6,41,42] In the case of a single $\pi$ bond, as in Figure 1a, there is only one QC state, which serves as the reference. However, in the case of the two $\pi$ bonds, in Figure 1b, there are two such reference states, $\Psi_{QC,2\pi}$ and $\Psi'_{QC,2\pi}$, which differ in the intrafragment spin relationship of the electrons in the mutually perpendicular p atomic orbitals (AOs) of the two fragments. Thus, in $\Psi_{QC,2\pi}$, the two electrons on either fragment have the same spin, and hence, the X/Y fragments enjoy exchange stabilization. On the other hand, in $\Psi'_{QC,2\pi}$, these electrons have opposite spins, and hence, this state is higher. To appreciate the need for these two states, we recall that upon spin-pairing of the two $\pi$ bonds as in $\Phi_{cov,2\pi}$ in Figure 1b, the spin in each AO will be 50% $\alpha$ and 50% $\beta$, and hence the proper reference state is the one having an average energy of the two QC states, $E_{QC,av}$, which takes into account this averaged spin situation. Therefore, we can determine the in situ $\pi$-bond energies as a difference between the energies of the complete VB wave function $\Psi_{VB}$ and the QC state, as follows in eq 3:

$$D_{n\pi} = D_{\mathrm{cov},n\pi} + \mathrm{RE_{cov\text{-}ion}}; n = 1,2 \tag{3a}$$

$$D_{\mathrm{cov},\pi} = E_{QC} + E_{\mathrm{cov},\pi}, n = 1 \tag{3b}$$

$$D_{\mathrm{cov},2\pi} = E_{\mathrm{QC,\,av}} + E_{\mathrm{cov},2\pi}, n = 2 \tag{3c}$$

Here, the quantities referring to the in situ bonding energies are labeled as $D$, to distinguish them from thermochemical bonding energies (BDE) that are usually calculated by taking the fragments apart.

*In situ Bond Energies and Driving Force for Bending.* As we outlined in the Introduction, in order to make meaningful comparisons across the periodic table and to retrieve trends in $\pi$ bond energies, all the molecules in the study were calculated at their linear geometries, although some of the molecules of the form H−X≡Y−H are of trans-bent geometries in their global minimum.[29−37] It should be emphasized that the linear geometries of those bent molecules are not random points on the PES but represent a saddle point of the second order. The establishment of intrinsic $\pi$-bond energies was then followed by determining the $\pi$-bond energies in the bent geometries and elucidating the driving forces for the distortion. Thus, the distortion energies of the $\sigma$ frame were determined by calculating $\Psi_{QC,2\pi}$ and $\Psi'_{QC,2\pi}$ at the linear and the trans-bent geometries. Similarly, calculating $D_\pi$ for each of the $\pi$ bonds in the linear and bent geometries provides the $\pi$ propensity for distortion. It is important to point out one caveat, namely, that the $\sigma$ and $\pi$ components in the bending plane actually mix and, hence, are not pure components. However, the variational optimization of the orbitals shows that even in the bent structures the $\sigma$ frame and $\pi$ bond retain these dominant characters and are in good accord with the conclusions of Kravchenko et al.[35] on the basis of solid

state $^{29}$Si NMR of the Sekiguchi compound. Therefore, the same set of VB structures is used in the present work for the VB description of linear as well as trans-bent molecules. The validity of this choice of VB structures is further established later in the text.

An important point to note is that the QC state remains nonbonding only at distances equal to or longer than the optimal bonding distance[43a] but becomes repulsive at shorter distances and therefore ceases to be a good reference state for gauging the in situ bonding energy. Accordingly, the method can be applied for the $\pi$ components of multiple bonds but will be much less accurate for the $\sigma$ component, since at a length of 1.25 Å the $\sigma$ bond is highly "compressed" relative to the optimal distance for a single $\sigma$ bond ($\sim$ 1.50 Å for a C−C $\sigma$ bond between sp hybrids). Thus, the in situ bonding energies for the $\sigma$ bonds will be estimated by a different mean, as will be detailed below.

**B. Analysis of the VB Wave Functions.** The weights, $w_i$, of the VB structures in the total wave function were determined by two methods. The first is the Coulson−Chirgwin method, which is the VB equivalent of the Mulliken population analysis, in eq 4:[44a]

$$w_i = c_i^2 + \sum_j c_i c_j S_{ij} \tag{4}$$

The second is the inverse overlap method[44b] in eq 5:

$$w_i \propto \frac{|c_i|^2}{(S^{-1})_{ii}}; \sum_i w_i = 1 \tag{5}$$

In both equations, the $S_{ii}$ or $S_{ij}$ terms are overlaps of VB configurations and $c_i$ is the coefficient of the $i$th VB structure in the wave function. Since the two methods gave very similar results, the following text shows only the Coulson−Chirgwin weights, while the inverse weights are relegated to the Supporting Information (Table S1).

**C. Computational Methods and Software.** The linear geometries of all structures in the study were optimized by CCSD(T)/6-31G* calculations. All CCSD(T) calculations were performed with the Gaussian 03 package.[45] VB calculations were performed on the optimized linear CCSD(T)/6-31G* geometries using the XMVB-0.1 package[46] with the same basis set.

The VB methods used in this study are VBSCF and BOVB. In both methods, the orbitals are divided into two sets: an active set, made of the orbitals involved in the $\pi$ central bonds, and an inactive set, involving the remaining orbitals. Core orbitals were excluded from VB calculations. The active $\pi$ orbitals are AOs or HAOs, while the inactive orbitals are doubly occupied molecular orbitals. All orbitals, active and inactive, are variationally optimized to minimize the energy of the ground state. Only active orbitals are kept strictly localized in the VB sense, while the inactive ones are allowed to freely delocalize. While in VBSCF[47] all (12) VB structures share the same set of orbitals, in BOVB,[48] each structure in the wave function has its own orbital set. This allows fluctuations in the size and shape of each set of orbitals due to local charge distribution in the different VB structures, thus introducing the incremental dynamic electron correlation, during bonding, into the wave function. The BOVB method was proved to be suitable for calculations of dissociation energies.[39b]

## III. RESULTS AND DISCUSSION

The various data are displayed in tables that are arranged in a matrix form, in order to highlight the trends as both atoms move from left to right and up and down the periodic table. Each matrix is divided into submatrices, corresponding to rows of the periodic table for atoms X and Y. In the 2,2 group, X and Y are both second row atoms; in 2,3, X is second row and Y is a third row atom; and so on. In order to compare triply bonded to bent HXYH structures, the ionic configurations, $X^-$, of atoms B, Al, and Ga are taken, so that they can make triple bonds while being bonded to H substituents. The other atoms are neutral. Atoms C, Si, and Ge also have H substituents, while N, P, and As do not. In all tables in the following discussion, all of the molecules are labeled as X≡Y, without implicit inclusion of the hydrogen substituents or of the formal negative charges.

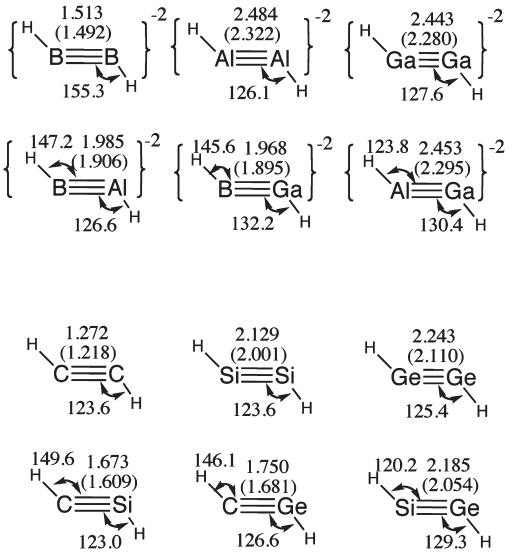


**Figure 2.** CCSD(T)/6-31G* optimized geometries for trans-bent molecules (distances in Å, angles in degrees). The bond lengths of the linear molecules are given in parentheses. The HCC angle in the trans-bent HC≡CH was fixed as in trans-bent HSi≡SiH while the CC distance was optimized.

**Geometries.** The CCSD(T)/6-31G* optimized geometries of all of the molecules are shown in Figure 2 and Table 1. Figure 2 shows the fully optimized geometries for the molecules involving B, Al, Ga, C, Si, and Ge atoms, which are the only molecules in this study that can undergo trans-bending. All of these molecules, with the exception of HCCH, are more stable in the trans-bent conformation than in the linear one. To get a bent geometry for HCCH, the HCC angle was fixed to the same value as the HSiSi angle in HSiSiH, and the CC bond length was optimized with this constraint. This enables us to estimate the CC bond lengthening due to bending.

Table 1 summarizes the data for the linear molecules. The trans bending lengthens the X≡Y distance in all cases, by widely different increments in the range 0.02−0.21 Å, where the maximal values correspond to the highest row combinations. The same trend is observed in the bending angles.

The origins of the distortion will be discussed in the end; right now, let us inspect the trends in the X≡Y distance for the linear molecules, as summarized in Table 1.

Table 1 shows the expected grouping of the bond lengths based on the location of the X and Y atoms in the periodic table. Molecules in the group (2,2) have the shortest X≡Y bond, while a sharp increase in the bond lengths is observed when moving to groups (2,3) and (2,4). The longest bond lengths are found in (3,3), (3,4), and (4,4), in agreement with the increased atomic size as one goes down the rows of the periodic table. Additionally,

**Table 1. CCSD(T)/6-31G* X≡Y Optimized Bond Lengths (in Å) for Linear Molecules**

| group | | 2 | | | 3 | | | 4 | | |
|---|---|---|---|---|---|---|---|---|---|---|
| | X/Y | $B^-$ | C | N | $Al^-$ | Si | P | $Ga^-$ | Ge | As |
| 2 | $B^-$ | 1.492 | | | | | | | | |
| | C | | 1.218 | | | | | | | |
| | N | | 1.172 | 1.120 | | | | | | |
| 3 | $Al^-$ | 1.906 | | | 2.322 | | | | | |
| | Si | | 1.609 | 1.597 | | 2.001 | | | | |
| | P | | 1.558 | 1.513 | | 1.984 | 1.921 | | | |
| 4 | $Ga^-$ | 1.895 | | | 2.294 | | | 2.280 | | |
| | Ge | | 1.681 | 1.691 | | 2.054 | 2.051 | | 2.110 | |
| | As | | 1.675 | 1.650 | | 2.087 | 2.035 | | 2.151 | 2.143 |

**Table 2. BOVB/6-31G* Calculated Weights of Covalent and Ionic Structures for a Single $\pi$-Bond in Triply Bonded X≡Y Molecules[a,b]**

| group | | 2 | | | 3 | | | 4 | | |
|---|---|---|---|---|---|---|---|---|---|---|
| | X/Y | $B^-$ | C | N | $Al^-$ | Si | P | $Ga^-$ | Ge | As |
| 2 | $B^-$ | **0.681** | | | | | | | | |
| | | *0.159* | | | | | | | | |
| | C | | **0.638** | | | | | | | |
| | | | *0.181* | | | | | | | |
| | N | | **0.631** | **0.625** | | | | | | |
| | | | *0.206* | *0.188* | | | | | | |
| | | | 0.164 | | | | | | | |
| 3 | $Al^-$ | **0.649** | | | **0.723** | | | | | |
| | | *0.290* | | | *0.139* | | | | | |
| | | 0.060 | | | | | | | | |
| | Si | | **0.659** | **0.654** | | **0.665** | | | | |
| | | | *0.168* | *0.132* | | *0.167* | | | | |
| | | | 0.173 | 0.214 | | | | | | |
| | P | | **0.652** | **0.652** | | **0.657** | **0.661** | | | |
| | | | *0.188* | *0.159* | | *0.218* | *0.169* | | | |
| | | | 0.159 | 0.189 | | 0.125 | | | | |
| 4 | $Ga^-$ | **0.650** | | | **0.717** | | | **0.707** | | |
| | | *0.275* | | | *0.120* | | | *0.146* | | |
| | | 0.075 | | | 0.163 | | | | | |
| | Ge | | **0.659** | **0.659** | | **0.667** | **0.663** | | **0.668** | |
| | | | *0.173* | *0.134* | | *0.177* | *0.132* | | *0.166* | |
| | | | 0.169 | 0.208 | | 0.155 | 0.205 | | | |
| | As | | **0.650** | **0.662** | | **0.660** | **0.669** | | **0.667** | **0.677** |
| | | | *0.196* | *0.166* | | *0.224* | *0.172* | | *0.214* | *0.162* |
| | | | 0.144 | 0.172 | | 0.115 | 0.159 | | 0.119 | |

[a] These are Coulson−Chirgwin weights (eq 4). [b] In each cell, the topmost value in bold corresponds to the weight of the covalent structure. The other values for the ionic structures are polarized in the directions X←Y (italics) and X→Y (regular font).

within each group, the bond lengths decrease generally upon moving from left to right in the periodic table (e.g., descending diagonals in each group). The exception is As≡As, which possesses a longer bond compared with Ge≡Ge.

In general, these CCSD(T)/6-31G* bond lengths are in good agreement with the triple bond covalent radii, calculated by Pyykkö at al.[49] These trends are expected since the X≡Y bond lengths are determined mainly by the underlying $\sigma$ bonds, which shrink along with the atomic radius from left to right of the periodic table due to the increase in electronegativity values. However, it is notable that within each period, moving from column 13 to column 14 ($B^-$→C, $Al^-$→Si, $Ga^-$→Ge) results in strong bond shortening, while the shortening is much less significant on transit from column 14 to column 15 (C→N, Si→P, Ge→As). One explanation is that the molecules with X,Y being $B^-$, $Al^-$, and $Ga^-$ bear adjacent negative charges, which repel each other and tend to lengthen the triple bond. However, this electrostatic effect only concerns column 13 of the periodic

Table 3. $D_\pi$ Bond Energies Calculated at the BOVB/6-31G* Level of Theory

| group | | 2 | | | 3 | | | 4 | | |
|---|---|---|---|---|---|---|---|---|---|---|
| | X/Y | $B^-$ | C | N | $Al^-$ | Si | P | $Ga^-$ | Ge | As |
| 2 | $B^-$ | 45.69 | | | | | | | | |
| | C | | 92.25 | | | | | | | |
| | N | | 106.87 | 124.18 | | | | | | |
| 3 | $Al^-$ | 34.12 | | | 20.22 | | | | | |
| | Si | | 57.32 | 59.68 | | 43.93 | | | | |
| | P | | 65.48 | 71.32 | | 46.59 | 51.29 | | | |
| 4 | $Ga^-$ | 34.76 | | | 20.77 | | | 21.16 | | |
| | Ge | | 53.51 | 53.69 | | 40.87 | 43.17 | | 38.08 | |
| | As | | 56.64 | 59.52 | | 41.77 | 45.19 | | 38.84 | 40.06 |

Table 4. $D_{2\pi}$ Bond Energies (in kcal/mol) Calculated at the BOVB/6-31G* Level of Theory

| group | | 2 | | | 3 | | | 4 | | |
|---|---|---|---|---|---|---|---|---|---|---|
| | X/Y | $B^-$ | C | N | $Al^-$ | Si | P | $Ga^-$ | Ge | As |
| 2 | $B^-$ | 94.68 | | | | | | | | |
| | C | | 185.15 | | | | | | | |
| | N | | 212.65 | 242.81 | | | | | | |
| 3 | $Al^-$ | 77.40 | | | 44.78 | | | | | |
| | Si | | 117.38 | 127.90 | | 90.35 | | | | |
| | P | | 131.89 | 142.91 | | 97.91 | 102.80 | | | |
| 4 | $Ga^-$ | 74.17 | | | 46.44 | | | 47.80 | | |
| | Ge | | 108.82 | 117.23 | | 84.48 | 86.80 | | 78.99 | |
| | As | | 113.45 | 119.33 | | 88.26 | 91.16 | | 82.32 | 81.14 |

table and does not explain the Ge≡Ge→As≡As lengthening, instead of the expected shortening. Here, another effect must be taken into account, the lone pair bond weakening effect (LPBWE) discovered by Sanderson[50] several decades ago. The LPBWE is due to overlap repulsion between the electrons of the lone pair(s) and the electrons that are coupled to a $\sigma$ bond. As such, the LPBWE weakens the covalent coupling in the $\sigma$ bond, resulting in bond lengthening. Since atoms of column 15 bear a lone pair while those of column 14 do not, the LPBWE explains the small bond shortenings from group (3,3) to group (4,4) and the Ge≡Ge→As≡As lengthening. We shall revisit this effect later.

**Weights of the Covalent and Ionic Components of the $\pi$ Bonds.** Table 2 collects the BOVB/6-31G* computed weights of the covalent and ionic structures for a single $\pi$ bond. It is seen that all of the bonds have dominant covalent characters. Moreover, as a general rule, bonds in the third and fourth rows are slightly more covalent than those of the second row. In each cell in the table, the covalent weight is the largest for group 13 and the smallest for group 15 (with, once again, an exception for Ge≡Ge→As≡As). The behavior is similar when the two $\pi$ bonds are considered, but since there are more structures, we relegate the data to the Supporting Information (Table S.2). Note that the VB structure in which both $\pi$ bonds are covalent remains the predominant one, even if its weight may be inferior to 50% (as a natural consequence of the fact that the total number of VB structures is larger in the two-bond VB description than in the single-bond one).

**In situ Bonding Energies for the $\pi$ Bond.** Table 3 displays $D_\pi$ and Table 4 displays $D_{2\pi}$ values calculated at the BOVB/6-31G* level. The VB computed $D_{2\pi}$ values are in good agreement with the trends calculated for group 14 by Frenking et al. using an energy decomposition method.[32b] An interesting relationship between the $D_\pi$ and $D_{2\pi}$ values is projected in Figure 3, which plots one over the other. It is seen that the slope of the correlation is close to 2, which means that the two $\pi$ bonds behave approximately as two independent bonds, which in turn shows the self-consistency of the VB results.

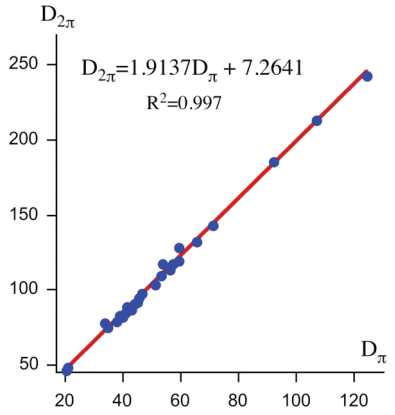


Figure 3. A plot of BOVB/6-31G* computed $D_\pi$ and $D_{2\pi}$ values.

Turning back to Tables 3 and 4, we note a few interesting patterns. As expected, the bond energy decreases down a column of the periodic table, with the unique exception of Ga≡Ga being slightly stronger than Al≡Al. The steepest decrease occurs in

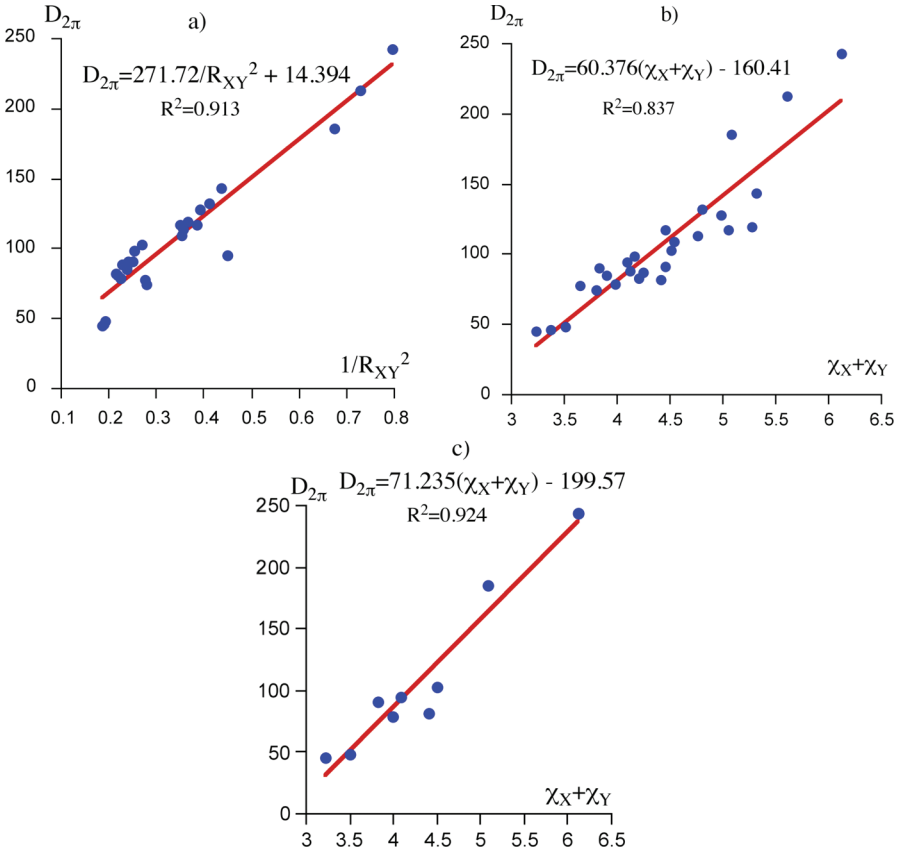


**Figure 4.** Plots of BOVB/6-31G* Computed $D_{2\pi}$ values against (a) the $1/R_{XY}^2$ values of the X≡Y molecules and (b) the molecular electronegativity, $\chi_X + \chi_Y$, for the set of 27 molecules. (c) The same plot as (b) but restricted to the homonuclear bonds.

**Table 5. The $D_{cov,2\pi}$ Portions (in kcal/mol) of $D_{2\pi}$ due to the Covalent VB Configuration, $\Phi_{cov}$**

| group | | 2 | | | 3 | | | 4 | | |
|---|---|---|---|---|---|---|---|---|---|---|
| | X/Y | $B^-$ | C | N | $Al^-$ | Si | P | $Ga^-$ | Ge | As |
| 2 | $B^-$ | 60.89 | | | | | | | | |
| | C | | 106.27 | | | | | | | |
| | N | | 115.33 | 129.69 | | | | | | |
| 3 | $Al^-$ | 35.52 | | | 28.51 | | | | | |
| | Si | | 60.67 | 53.71 | | 49.40 | | | | |
| | P | | 65.59 | 65.53 | | 46.40 | 47.71 | | | |
| 4 | $Ga^-$ | 36.84 | | | 28.75 | | | 28.92 | | |
| | Ge | | 56.09 | 48.50 | | 47.52 | 45.41 | | 44.53 | |
| | As | | 56.71 | 52.32 | | 42.50 | 42.71 | | 40.66 | 37.87 |

going from the second- to the third-row bond, and thereafter the decrease is moderate. Another clear tendency from both Tables 3 and 4 is a strengthening of the $\pi$ bond(s) as one moves from left to right in a given period, hence suggesting a relationship between bond strength and electronegativity. A comparison of Tables 3 and 4 with Table 1 also shows a relationship between $\pi$-bonding strength and interatomic distance: the shorter the bond, the stronger. These trends are summarized in Figure 4: Figure 4a shows that there is a linear correlation between the $D_{2\pi}$ values and the inverse of the squared X≡Y bond lengths. Actually, these latter quantities are related to electronegativities if one uses the definition of Allred and Rochow[51] for the electronegativities of atoms, eq 6:

$$\chi \propto Z_{eff}/R^2 \qquad (6)$$

Here, $R$ is the atomic radius and $Z_{eff}$ is the effective nuclear charge of the atom in question.[51] By this definition, the electronegativity measures the attractive force of the nuclei on the valence electrons. Extending this reasoning, one would deduce that the larger the electronegativity, the stronger the force exerted on the valence electrons of a neighboring atom and the stronger the bond between the two atoms. It is therefore logical to expect a correlation between the $D_\pi$ or $D_{2\pi}$ values with the

Table 6. The Covalent−Ionic Resonance Energy Components of $D_{2\pi}$, in kcal/mol

| group | | 2 | | | 3 | | | 4 | | |
|---|---|---|---|---|---|---|---|---|---|---|
| | X/Y | $B^-$ | C | N | $Al^-$ | Si | P | $Ga^-$ | Ge | As |
| 2 | $B^-$ | 33.79 | | | | | | | | |
| | C | | 78.88 | | | | | | | |
| | N | | 97.32 | 113.12 | | | | | | |
| 3 | $Al^-$ | 41.88 | | | 16.27 | | | | | |
| | Si | | 56.71 | 74.19 | | 40.95 | | | | |
| | P | | 66.30 | 77.38 | | 51.51 | 55.09 | | | |
| 4 | $Ga^-$ | 37.33 | | | 17.69 | | | 18.88 | | |
| | Ge | | 52.73 | 68.73 | | 36.96 | 41.39 | | 34.46 | |
| | As | | 56.74 | 67.01 | | 45.76 | 48.45 | | 41.66 | 43.27 |

sum of electronegativities of X and Y, i.e., the "*molecular electronegativity*". Such a correlation is indeed observed for the whole set of 27 molecules under study (Figure 4b), with a better correlation coefficient (0.92) when the homonuclear bonds are considered alone (Figure 4c).

Such a correlation between in situ $\pi$-bond strengths and molecular electronegativity had already been mentioned by some of us in a study of double bonds in the second and third rows.[38a,39] In $\sigma$ bonds, the same trend is observed from Li−Li to C−C but breaks down from N−N to F−F. This irregular behavior is due to the LPBWE discussed by Sanderson[50] and already mentioned above. The LPBWE weakens the $\sigma$ bonds but has no direct effect on $\pi$ bonds. Indeed, if the LPBWE is removed in model calculations, the so-estimated "unweakened" $\sigma$ bonds show the expected linear increase from Li−Li to F−F.[52] Thus, the linear correlation shown in Figure 4 for $\pi$ bonding energies with molecular electronegativity represents a physically meaningful relationship, which in $\sigma$ bonds applies only to the hypothetical "unweakened" bonds.[52]

**Components of the $\pi$-Bonding Energies.** In eq 3a, above, the total bonding energy $D_{2\pi}$ for the two $\pi$ bonds was expressed as a sum of two components, the $D_{cov,2\pi}$ component and $RE_{cov\text{-}ion}$, the covalent−ionic resonance energy. These quantities are collected in Tables 5 and 6.

The $D_{cov,2\pi}$ values in Table 5 among the different groups show nearly the same trends as the $D_\pi$ and $D_{2\pi}$ values. The strengths of the covalent interactions generally decrease as one moves down the periodic table, especially from the second row to the third row. On the other hand, the $D_{cov,2\pi}$ values for the homonuclear bonds increase in each group as one goes from left to right of the periodic table. As we argued above, this trend follows the order of molecular electronegativities, which in turn reflect the attractive force of the nuclei on the valence electrons (vide supra, eq 6). There are however two exceptions, the *decrease* of $D_{cov,2\pi}$ from Ge≡Ge to As≡As and from Si≡Si to P≡P. Here, we recall that the As≡As bond was found to be longer than the Ge≡Ge one (Table 1), as a consequence of the lengthening effect of the LPBWE on the $\sigma$ bond in As≡As. This, together with the fact that the $\pi$ orbitals are necessarily more compact in As than in Ge easily explains that the covalent interaction is weaker in As≡As than in Ge≡Ge. Thus, the As≡As exception in the trends of homonuclear bonds in Table 5 is an indirect consequence of the LPBWE on the $\sigma$ bonds. The same kind of explanation holds for the unexpected decrease of $D_{cov,2\pi}$ from Si≡Si to P≡P.

Table 6 shows the $RE_{cov\text{-}ion}$ values, due to the mixing of the ionic structures into the covalent structures, obtained at the BOVB/6-31G* level. An inspection of Table 6 shows that unlike Pauling's scheme,[53] wherein it is assumed that for homonuclear bonds $RE_{cov\text{-}ion}$= 0, the present BOVB calculations show that these bonds possess very large covalent−ionic resonance energies, and the same is true for many of the other bonds in Table 6.

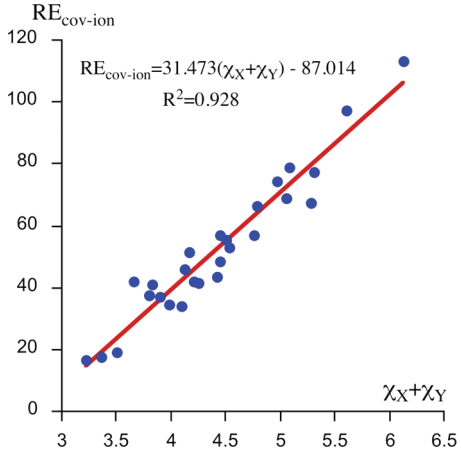


**Figure 5.** A plot of $RE_{cov\text{-}ion}$ vs the molecular-electronegativity value of the bond constituents.

Figure 5 demonstrates that the molecular-electronegativity values ($\chi_X + \chi_Y$) nicely organize the $RE_{cov\text{-}ion}$ quantities for all 27 bonds. By contrast, the plot against the electronegativity difference, $\chi_X - \chi_Y$, has a very poor correlation ($r^2$ = 0.17, see Figure S1). Once again, this result is not in accord with the Pauling scheme,[53] wherein the $RE_{cov\text{-}ion}$ values are determined solely by the electronegativity differences.

The correlation of $RE_{cov\text{-}ion}$ with the molecular electronegativity is a fundamental relation, which is associated with the mechanism of bonding. When atoms (fragments) enter into bonding, their orbitals shrink. This shrinkage lowers the potential energy ($V$) of the atoms (fragments) but raises much more steeply their kinetic energies ($T$),[43] and this disrupts the virial ratio $T/V$ which has to be −0.5 in equilibrium. As such, resonance energy is required to lower the kinetic energy and restore the equilibrium $T/V$ ratio. When the orbitals are to begin with quite compact, as in electronegative atoms, orbital shrinkage causes too much of a kinetic energy increase, and this is further aggravated when the atoms (fragments) bear lone pairs, which raise the kinetic energy due to Pauli repulsion between them and as well as with the bonding electron. *What lowers the kinetic energy*

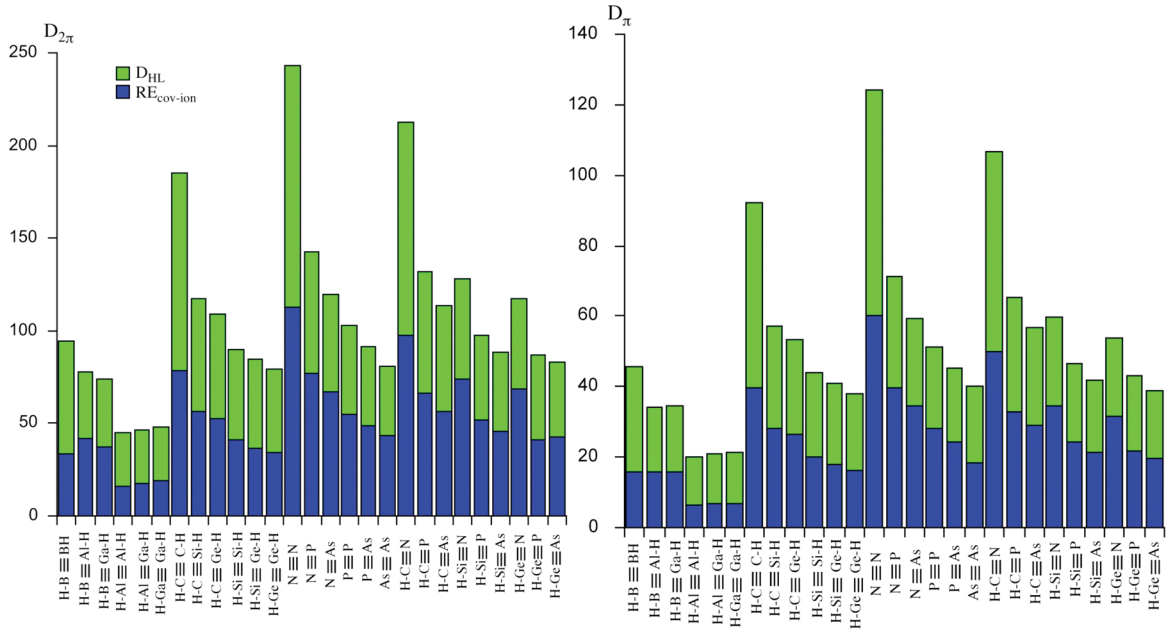


**Figure 6.** Diagram plots showing the $D_{cov}$ (green) and $RE_{cov\text{-}ion}$ (blue) components of $D_{2\pi}$ (left side) and $D_{\pi}$ (right side).

*and restores the virial ratio to its equilibrium value is the covalent—ionic resonance energy due to the admixture of the ionic structures into the covalent structure*; the more compact the atoms and the more lone pairs they have, the larger the resonance energy[39a] that is required to restore the virial ratio. It follows that the molecular electronegativity, which is associated with either orbital compactness or the presence of lone pairs or both, favors large covalent—ionic resonance energies. This tendency, which has been demonstrated for single bonds,[39e] has also been seen to be valid for the $\pi$ components of double bonds.[38a]

Figure 6 shows diagrammatically the total $\pi$-bond energy, and its breakdown into covalent and resonance energy contributions for both $D_{\pi}$ (right side) and $D_{2\pi}$ (left side). It is apparent that, whether for one-bond or for two-bond calculations, the quantity $RE_{cov\text{-}ion}$ is always significant, and in about half of the bonds, it is either close to or more than 50% of the total bonding energy. These bonds were shown by us before to form a special family of bonds, the so-called charge-shift (CS) bonds.[39] Interestingly, most of the $\pi$-CS bonds in the set of 27 molecules are found when at least one of the bonded atoms involves a lone pair, e.g., in Si≡N, Ge≡N, N≡P, P≡P, As≡As, etc. This nicely illustrates the relationship between CS bonding and the presence of lone pairs in the bonded atoms, as mentioned above. It follows that the increase of $\pi$-$RE_{cov\text{-}ion}$ due to the presence of lone pair(s) compensates partially the LPBWE of the $\sigma$ bonds by the same lone pairs. As an outcome, the total bonding energies of the $\pi$ bonds, $D_{\pi}$ or $D_{2\pi}$, always increase in a given group as the bonded atoms are taken from the left to the right of the periodic table (see also Table S3 and Figure S2 in the Supporting Information).

**The Distortion Energies of HX≡YH from Linear to Trans-Bent Forms.** As can be seen in Table 1, part of the triple bonds, those containing atoms in rows higher than 2 and those involving group 13 and 14 atoms, undergo trans bending. By contrast, HC≡CH and HC≡CN remain linear. Following our preliminary study,[37] we analyzed this propensity or lack thereof as a balance between the $\sigma$ and $\pi$ propensities, $\Delta E_{\sigma}$ and $\Delta E_{\pi}$. As commented upon above, such an analysis is valid if the linear and trans-bent forms of the molecule can be described by the same set of VB structures, having in each case a $\sigma$ bond along the X—Y axis, and either a pair of degenerate $\pi$ bonds off axis (in the linear) or an out-of plane $\pi$ bond and an in-plane pseudo-$\pi$ bond (in the bent). This choice of common VB structure set for the linear and bent molecule was tested by comparing the VB-calculated total distortion energies to the corresponding CCSD(T) values. The results collected in Table 7 show that VB theory predicts the distortive propensity of those molecules, which prefer the trans-bent structure. It also reveals a fair agreement between the VB and CCSD(T) sets of values, demonstrating that the VB calculations treat the linear and bent forms on equal footing and can therefore form a basis for the following discussion. Quantitative deviations between VB and CCSD(T) distortion energies may reflect that, in some cases of, e.g., the polar

**Table 7. Comparison of VB and CCSD(T) Distortion Energies (kcal/mol)[a]**

| | CCSD(T) | VBSCF | BOVB |
|---|---|---|---|
| $(HB{\equiv}BH)^{-2}$ | 2.90 | 0.81 | 2.08 |
| $(HB{\equiv}AlH)^{-2}$ | 7.88 | 11.28 | 9.38 |
| $(HB{\equiv}GaH)^{-2}$ | 5.90 | 9.70 | 8.1 |
| $(HAl{\equiv}AlH)^{-2}$ | 18.18 | 22.97 | 22.2 |
| $(HAl{\equiv}GaH)^{-2}$ | 17.57 | 23.58 | 23.11 |
| $(HGa{\equiv}GaH)^{-2}$ | 16.52 | 23.84 | 23.36 |
| HC≡CH | −25.33 | −25.85 | −26.29 |
| HC≡SiH | 9.06 | 13.41 | 18.44 |
| HC≡GeH | 9.11 | 14.22 | 16.24 |
| HSi≡SiH | 23.55 | 30.62 | 28.86 |
| HSi≡GeH | 23.75 | 30.82 | 29.00 |
| HGe≡GeH | 24.09 | 31.77 | 29.79 |

[a] The bending energies are calculated as the energy differences between geometry-optimized bent and linear structures, as displayed in Figure 2 and Table 1, respectively.


dx.doi.org/10.1021/ct100741b |*J. Chem. Theory Comput.* 2011, 7, 955–968

**Scheme 4. Definition of the $\sigma$-Propensity for Trans Bending of HX≡YH Bonds**

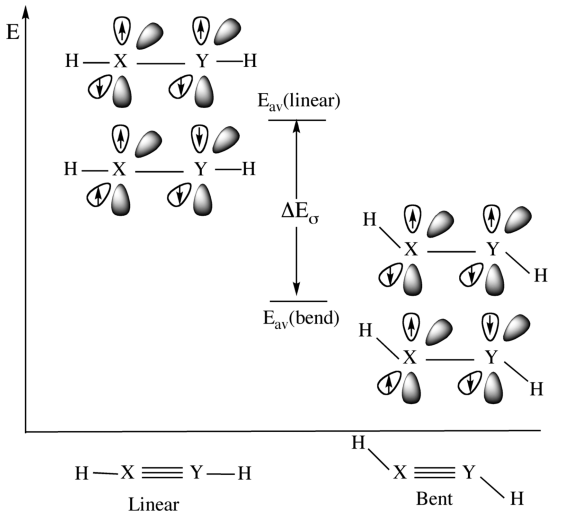


molecules of the heavier elements, the description of the bending process may require more structures.

**The Driving Force for Trans Bending.** Since the QC states are devoid of $\pi$ bonds, the bending energy of the QC state will yield the $\sigma$ propensity of the molecule to prefer a bent or linear structure, $\Delta E_\sigma$. As shown in Scheme 4, the $\Delta E_\sigma$ values were calculated from the average energies of the QC states in the linear and bent geometries.

Table 8 shows the so calculated quantities for all of the molecules that can undergo trans bending, i.e., HX≡XY with X,Y belonging to groups 13 and 14. Recall that for HC≡CH, which is linear at equilibrium, we fixed the bending angle for the bent structure as in HSi≡SiH (123°) and reoptimized the geometry with this constraint (Figure 2).

It is seen that the bonding energy of the out-of-plane $\pi$ bond, $D_{\pi\text{-out}}$, is hardly affected by bending and varies within only a few kcal/mol. On the other hand, as can be seen from the variations of $D_{\pi\text{-in}}$, upon bending the in-plane pseudo-$\pi$ bonds become significantly weaker in the trans-bent isomers than in the linear ones. The weakening is especially important in molecules involving atoms of group 14 (13−40 kcal/mol), and much less so in group 13 compounds (4−8 kcal/mol). As a consequence, the total bonding energy of both $\pi$ bonds ($D_{\pi\text{-in}} + D_{\pi\text{-out}}$) decreases upon bending in all cases, by 6 to 46 kcal/mol.

By contrast to the $\pi$ bonds, as shown by the positive $\Delta E_\sigma$ in Table 8, the $\sigma$ frame is invariably stabilized by the trans bending. Further, the $\Delta E_\sigma$ values are all significant, ranging from 20 to 56 kcal/mol for group 14 and from 10 to 31 kcal/mol for group 13 compounds. Thus, all of the $\sigma$ frames, including the one of acetylene, prefer the bent structure, which strengthens $\sigma$ bonding. However, in all molecules displayed in Table 8, except for acetylene, this $\sigma$-bond strengthening overrides the $\pi$-bond weakening, thereby leading to trans bending. The $\sigma$ propensity to distort increases for the higher row atoms, while the loss of $\pi$-bonding energy decreases in the same direction. Consequently, acetylene remains linear, despite the distortive propensity of its $\sigma$ frame, while all other HX≡YH molecules undergo trans bending. Inspection of the $\pi$-bond energy trends reveals that the in-plane bond is reduced to about 50% of its original strength in the linear structure when X and Y belong to group 14. Hence, in agreement with previous experimental and theoretical studies,[23,35,37] the formal number of bonds in these molecules is approximately $2^1/_2$.

The root cause for $\pi$-bond weakening upon distortion is obviously due to the loss of overlap between the AOs involved in the in-plane pseudo-$\pi$ bond as trans-bending takes place. On the other hand, the $\sigma$-bond strengthening can be due to several causes. One obvious factor is bond-length relaxation in trans-bent structures relative to linear ones (compare Figure 2 to Table 1). Thus, the bond distance between the heavy atoms is too short in the linear structure for an optimal $\sigma$ bond. Trans-bending lengthens the distance between heavy atoms, leading somewhat to $\sigma$-bond strengthening. Additionally, VB calculations using the spin−coupled method have shown that hyperconjugation also contributes to $\Delta E_\sigma$, albeit in a minor way.[37] However, the most important factor for $\sigma$-bond strengthening upon bending has been shown, in a few examples (X, Y = C, Si), to be related to the increase of s orbital participation in bonding through rehybridization.[34,37] Thus, the increase in s orbital population is 0.044 $e^-$ for HC≡CH, 0.262 $e^-$ for HSi≡CH, and 0.604 $e^-$ for HSi≡SiH,[37] which correlates well with the $\Delta E_\sigma$ values 20, 40, and 56 kcal/mol in this series. This last effect follows the pioneering reasoning of Trinquier and Malrieu,[40a,b] that the trans bent geometries of analogous doubly bonded molecules is due to the tendency of the molecular fragments to keep as much as possible their ground state and avoid the costly electronic promotion to the high-spin triplet states.

**An Overview of $\sigma$ and $\pi$ Bonding in Triply Bonded HX≡YH Molecules.** The above energy separation allows us to compute the individual $\sigma$- and $\pi$-bonding contributions to the triply bonded molecules from the corresponding BDEs of the various molecules relative to the open-shell dissociated fragments. In the following approach, used before,[32b,40,54] the HX≡YH molecule is considered as the product of interactions between two XH +YH fragments in their open shell $^4\Sigma^-$ states, which in most cases are the excited states of the fragments. The net dissociation energy $BDE_{\sigma+2\pi}$ is obtained after adding the demotion energy of the fragments from $^4\Sigma^-$ to their ground states $^2\Pi$. Thus, the dissociation process is decomposed into two formal steps, eqs 7 and 8:

$$HX{\equiv}YH \rightarrow HX(^4\Sigma^-) + HY(^4\Sigma^-); \Delta E = D_{\text{total}} \quad (7)$$

$$HX(^4\Sigma^-) + HY(^4\Sigma^-) \rightarrow HX(^2\Pi) + HY(^2\Pi)]; \quad \Delta E = -E_{\text{prom}} \quad (8)$$

where $E_{\text{prom}}$ is the promotion energy required to excite a fragment from its $^2\Pi$ state to its $^4\Sigma$ state. Since the actual dissociation process, from the molecule to the fragments in their ground states, is the sum of reactions 7 and 8 and corresponds to the bond dissociation energy $BDE_{\sigma+2\pi}$, we can obtain $D_{\text{total}}$ from eq 9:

$$D_{\text{total}} = BDE_{\sigma+2\pi} + E_{\text{prom}} \quad (9)$$

It is then a simple task to extract the $\sigma$ contribution to bonding, $D_\sigma$, by subtracting the $\pi$ contribution, $D_{2\pi}$, from $D_{\text{total}}$:

$$D_\sigma = D_{\text{total}} - D_{2\pi} \quad (10)$$

Table 9 displays some $BDE_{\sigma+2\pi}$ values calculated at the B3LYP/6-31G* level for a series of HX≡XY molecules with X, Y belonging to group 14. From these values, the total bond

**Table 8. $\sigma$ and $\pi$ Driving Forces for Bending Away from Linear HX≡YH Molecules**

| | Bond Energies (kcal/mol) | | | | | |
|---|---|---|---|---|---|---|
| | $(H-B\equiv B-H)^{-2}$ | | $(H-B\equiv Al-H)^{-2}$ | | $(H-Ga\equiv Ga-H)^{-2}$ | |
| | linear | bent | linear | bent | linear | bent |
| $D_{\pi\text{-out}}$ | 45.69 | 45.81 | 34.12 | 29.80 | 21.16 | 18.33 |
| $D_{\pi\text{-in}}$ | 45.69 | 37.76 | 34.12 | 26.71 | 21.16 | 17.53 |
| $(D_{\pi\text{-in}} + D_{\pi\text{-out}})$ | 91.38 | 83.57 | 68.24 | 56.51 | 42.32 | 35.86 |
| $\Delta E_\pi$ | −7.81 | | −11.73 | | −6.46 | |
| $\Delta E_\sigma$ | +9.89 | | +21.11 | | +29.82 | |
| | $(H-B\equiv Ga-H)^{-2}$ | | $(H-Al\equiv Al-H)^{-2}$ | | $(H-Al\equiv Ga-H)^{-2}$ | |
| | linear | bent | linear | bent | linear | bent |
| $D_{\pi\text{-out}}$ | 34.76 | 31.31 | 20.22 | 17.19 | 20.77 | 17.90 |
| $D_{\pi\text{-in}}$ | 34.76 | 27.11 | 20.22 | 14.12 | 20.77 | 16.35 |
| $(D_{\pi\text{-in}} + D_{\pi\text{-out}})$ | 69.52 | 58.42 | 40.44 | 31.31 | 41.54 | 34.25 |
| $\Delta E_\pi$ | −11.1 | | −9.13 | | −7.29 | |
| $\Delta E_\sigma$ | 19.20 | | 31.33 | | 30.40 | |
| | H−C≡C−H | | H−C≡Si−H | | H−Ge≡Ge−H | |
| type | linear | bent | linear | bent | linear | bent |
| $D_{\pi\text{-out}}$ | 92.25 | 86.44 | 57.32 | 56.03 | 38.08 | 32.83 |
| $D_{\pi\text{-in}}$ | 92.25 | 52.01 | 57.32 | 37.19 | 38.08 | 24.94 |
| $(D_{\pi\text{-in}} + D_{\pi\text{-out}})$ | 184.50 | 138.45 | 114.64 | 93.22 | 76.16 | 57.77 |
| $\Delta E_\pi$ | −46.05 | | −21.42 | | −18.39 | |
| $\Delta E_\sigma$ | 19.76 | | 39.86 | | 48.18 | |
| | H−Si≡Si−H | | H−C≡Ge−H | | H−Si≡Ge−H | |
| type | linear | bent | linear | bent | linear | bent |
| $D_{\pi\text{-out}}$ | 43.93 | 37.08 | 53.51 | 51.46 | 40.87 | 34.95 |
| $D_{\pi\text{-in}}$ | 43.93 | 23.88 | 53.51 | 36.12 | 40.87 | 24.58 |
| $(D_{\pi\text{-in}} + D_{\pi\text{-out}})$ | 87.86 | 60.96 | 107.02 | 87.58 | 81.74 | 59.53 |
| $\Delta E_\pi$ | −26.9 | | −19.44 | | −22.21 | |
| $\Delta E_\sigma$ | 55.76 | | 35.68 | | 51.21 | |

[a] $\Delta E_\pi = (D_{\pi\text{-in}} + D_{\pi\text{-out}})_{\text{Bent}} - (D_{\pi\text{-in}} + D_{\pi\text{-out}})_{\text{Linear}}$; $\Delta E_\sigma = E_{\text{QC,av}}(\text{bent}) - E_{\text{QC,av}}(\text{linear})$. Negative values mean that the bonding is weakened upon trans bending and vice versa for positive values.

**Table 9. Estimations of the Respective Bond Strengths of the $\sigma$ and $\pi$ Components of the Triple Bond in HX≡YH Species, in Their Bent and Linear Conformations (All Energies in kcal/mol)**

| | $BDE_{\sigma+2\pi}$[a] | | $E_{\text{prom}}$[b] | $D_\sigma$[c] | | $D_{2\pi}$[d] | |
|---|---|---|---|---|---|---|---|
| | bent | linear | | bent | linear | bent | linear |
| HC≡CH | 201.38 | 231.18 | 40.38 | 103.31 | 87.06 | 138.45 | 184.50 |
| HSi≡SiH | 57.52 | 35.40 | 85.56 | 82.12 | 33.10 | 60.96 | 87.86 |
| HGe≡GeH | 50.77 | 22.26 | 95.68 | 88.68 | 41.78 | 57.77 | 76.16 |
| HGe≡CH | 99.66 | 91.23 | 68.03 | 80.11 | 52.24 | 87.58 | 107.02 |
| HGe≡SiH | 53.65 | 28.56 | 90.62 | 84.74 | 37.44 | 59.53 | 81.74 |
| HSi≡CH | 113.59 | 106.63 | 62.97 | 83.34 | 54.96 | 93.22 | 114.64 |

[a] Bond dissociation energies calculated at the B3LYP/6-31G* level. [b] Experimental ($^2\Pi \rightarrow {}^4\Sigma^-$) promotion energies, eq 8. [c] Equation 10 [d] $D_{2\pi}$ values were calculated as a sum of $D_{\pi\text{-in}} + D_{\pi\text{-out}}$ energies.

strengths $D_{\text{total}}$ are estimated through eq 9 by using experimental promotion energies $D_{\text{prom}}$. Finally, the $D_\sigma$ values are estimated through eq 10. It can be seen that in all linear conformations, the $\sigma$ contribution to bonding, $D_\sigma$, is slightly less than one-third of the total, i.e., smaller than each of the $\pi$ contributions. On the other hand, $D_\sigma$ is clearly the strongest component of the triple bond for bent molecules.

## CONCLUSION

With an aim of establishing insight into the trends in bonding and structure in a surging field of multiple bonding,[7d,29e,30,33,35,36] we describe in this paper a valence bond (VB) study of 27 triply bonded molecules of the general type X≡Y, where X and Y are main element atoms and/or fragments from groups 13−15 in the periodic table. The molecules were studied in their linear as well as bent geometries, wherever such bending occurs (e.g., in group 14). The VB method allows the separation of $\pi$ and $\sigma$ bonding and thereby leads to the following conclusions:

(a) Both the single $\pi$-bond energy as well as the total $\pi$-bonding energy for the entire set correlate with the "*molecular electronegativity*", which is the sum of the X


dx.doi.org/10.1021/ct100741b |*J. Chem. Theory Comput.* 2011, 7, 955–968

and Y electronegativites for X≡Y. Thus, the more electronegative the X and Y fragments, in a given triply bonded molecule, the stronger the two $\pi$ bonds. The electronegativity difference is much less important. The correlation with the molecular electronegativity enables us to establish a simple rule of periodicity: Thus, following the order of the molecular electronegativity, $\pi$-bonding strength generally increases from left to right in a period and decreases down a column in the periodic table.

(b) It was found that invariably the $\sigma$ frame prefers trans bending, while $\pi$ bonding is destabilized and opposes this distortion. In HC≡CH, the $\pi$-bonding destabilization overrides the propensity of the $\sigma$ frame to distort, while in the higher row molecules, the $\sigma$ frames win out and establish trans-bent molecules with $2^1/_2$ bonds, in accord with recent experimental evidence based on solid state $^{29}$Si NMR of the Sekiguchi compound.[35] Thus, as concluded before,[34,37] the trans-bent molecules are cases where "less bonds pay more". The distortive propensity of the $\sigma$ frame originates in the increase of the s-atomic orbital population, which lowers the promotion energy ($^2\Pi \rightarrow {}^4\Sigma^-$) of the fragments within the molecule.

(c) The separation of the $\sigma$ frame and $\pi$ bonding allows one to determine the corresponding $\sigma$- and $\pi$-bond energies (Table 9). The trends in the $\sigma$-bond energies also follow the molecular electronegativity and increase by bending by approximately 16−49 kcal/mol for the molecules studied here.

(d) All of the $\pi$ bonds were found to have significant contributions from the resonance energy due to covalent−ionic mixing ($RE_{cov\text{-}ion}$). The $RE_{cov\text{-}ion}$ quantity for all 27 molecules correlates linearly with the corresponding molecular electronegativity, and this correlation is rooted in the bonding mechanism and the establishment of the virial ratio that typifies the equilibrium condition.[39,43] The $\pi$-bonding energy of the more electronegative fragments has a dominant $RE_{cov\text{-}ion}$ contribution which exceeds 50% of the total bonding. Hence, all of the triple bonds have significant charge-shift character,[39,42] and those having high molecular electronegativity are charge-shift bonds, wherein bonding is dominated by the resonance energy of the covalent and ionic forms, rather than by either form by itself.

## ■ ASSOCIATED CONTENT

**Supporting Information.** Scheme with covalent and ionic structures for two $\pi$ bonds (Scheme S1), a plot of $RE_{cov\text{-}ion}$ vs the absolute difference in molecular-electronegativity value of the bond constituents (Figure S1), BOVB/6-31G* inverse weights of covalent and ionic structures for a single $\pi$ bond (Table S1), BOVB/6-31G* calculated weights (eq 4) of covalent structures for two $\pi$ bonds (Table S2), a table of the $RE_{cov\text{-}ion}/D_{n\pi}$ ratio for one or two bonds Table S3, Cartesian coordinates (Table S4), and a figure of the correlation between the quantities (Figure S2). This information is available free of chage via the Internet at http://pubs.acs.org/.

## ■ AUTHOR INFORMATION

### Corresponding Author

*(P.H.) Phone: +33-1-69156175. Fax: +33-1-69154447. E-mail: philippe.hiberty@u-psud.fr. (S. S.) Phone: +972-2-6585909. Fax: +972-2-6584680. E-mail: sason@yfaat.ch.huji.ac.il.

## ■ ACKNOWLEDGMENT

S.S. thanks the Israeli Science Foundation for a grant (ISF 53/09).

## ■ REFERENCES

(1) (a) Brock, W. H. *The Norton History of Chemistry*; Norton W.W. & Co.: New York, 1992, pp 241−269; 465−483. (b) Frenking, G.; Shaik, S. *J. Comput. Chem.* **2007**, *28*, 1–3.

(2) (a) Kipping, F. S. *Proc. R. Soc.* **1911**, *27*, 143. (b) Kipping, F. S. *J. Chem. Soc., Trans.* **1923**, *123*, 2590–2597. (c) Kipping, F. S. *J. Chem. Soc., Trans.* **1924**, *125*, 2291–2297. (d) Kipping, F. S. *Proc. R. Soc. London* **1937**, *159*, 139–148.

(3) Jutzi, P. *Angew. Chem., Int. Ed. Engl.* **1975**, *14*, 232–245.

(4) Pitzer, K. S. *J. Am. Chem. Soc.* **1948**, *70*, 2140–2145.

(5) Mulliken, R. S. *J. Am. Chem. Soc.* **1950**, *72*, 4493–4503.

(6) Kutzelnigg, W. *Angew. Chem., Int. Ed. Engl.* **1984**, *23*, 272–295.

(7) For metal−metal bonding, see for example: (a) CrCr quintuple bond in Hsu, C. W.; Yu, J. S. K.; Yen, C. H.; Lee, G. H.; Wang, Y.; Tsai, Y. C. *Angew. Chem., Int. Ed.* **2008**, *47*, 9933–9936.(b) Slighi-Dumetrescu, I.; Petrar, P.; Neme, G.; King, R. B. "Theoretical Aspects of Main Group Multiple Bonded Systems. In *Computational Bioinorganic and Inorganic Chemistry*; Solomon, E. I., Scott, R. A., King, R. B., Eds.; John-Wiley & Sons: New York, 2009; pp 563−575. (c) McGrady, J. E. Electronic Sturcture of Metal−Metal Bonds. In *Computational Bioinorganic and Inorganic Chemistry*; Solomon, E. I., Scott, R. A., King, R. B., Eds.; John-Wiley & Sons: New York, 2009; pp 425−432. (d) Xu, B.; Li, Q.-S.; Xie, Y.; King, R. B.; Schaefer, H. F., Jr. *J. Chem. Theory Comput.* **2010**, *6*, 735–746. (e) Frenking, G.; von Hopffgarten, M. Calculation of Bonding Properties. In *Computational Bioinorganic and Inorganic Chemistry*; Solomon, E. I., Scott, R. A., King, R. B., Eds.; John-Wiley & Sons: New York, 2009; pp 3−15.

(8) Yoshifuji, M.; Shima, I.; Inamoto, N.; Hirotsu, K.; Higuchi, T. *J. Am. Chem. Soc.* **1981**, *103*, 4587–4589.

(9) Brook, A. G.; Abdesaken, F.; Gutekunst, B.; Gutekunst, G.; Kallury, R. K. *Chem. Commun* **1981**, 191–192.

(10) West, R.; Fink, M. J. *Science* **1981**, *214*, 1343–1344.

(11) West, R. *Angew. Chem., Int. Ed. Engl.* **1987**, *26*, 1201–1211.

(12) Power, P. P. *Chem. Rev.* **1999**, *99*, 3463–3504.

(13) Regitz, M. *Chem. Rev.* **1990**, *90*, 191–213.

(14) (a) Becker, G.; Gresser, G.; Uhl, W. *Z. Naturforsch., B: Chem. Sci.* **1981**, *36*, 16–19. (b) Gier, T. E. *J. Am. Chem. Soc.* **1961**, *83*, 1769–1770.

(15) (a) Zhou, M.; Tsumori, N.; Li, Z.; Fan, K.; Andrews, L.; Xu, Q. *J. Am. Chem. Soc.* **2002**, *124*, 12936–12937. (b) Zhou, M. F.; Jiang, L.; Xu, Q. *Chem.—Eur. J.* **2004**, *10*, 5817–5822.

(16) (a) Mennekes, T.; Paetzold, P.; Boese, R. *Angew. Chem., Int. Ed. Engl.* **1990**, *29*, 899–900. (b) Grigsby, W. J.; Power, P. P. *J. Am. Chem. Soc.* **1996**, *118*, 7981–7988.

(17) (a) Su, J.; Li, X.-W.; Crittendon, R. C.; Robinson, G. H. *J. Am. Chem. Soc.* **1997**, *119*, 5471–5472. (b) Xie, Y.; Grev, R. S.; Gu, J.; Schaefer, H. F.; Schleyer, P. v. R.; Su, J.; Li, X.-W.; Robinson, G. H. *J. Am. Chem. Soc.* **1998**, *120*, 3773–3780.

(18) (a) Cotton, F. A.; Cowley, A. H.; Feng, X. *J. Am. Chem. Soc.* **1998**, *120*, 1795–1799. (b) Grunenberg, J. R.; Goldberg, N. *J. Am. Chem. Soc.* **2000**, *122*, 6045–6047. (c) Molina, J. M.; Dobado, J. A.; Heard, G. L.; Bader, R. F. W.; Sundberg, M. R. *Theor. Chem. Acc.* **2001**, *105*, 365–373.

(19) Hunold, R.; Allwohn, J.; Baum, G.; Massa, W.; Berndt, A. *Angew. Chem., Int. Ed. Engl.* **1988**, *27*, 961–963.

(20) Karni, M.; Apeloig, Y.; Schröder, D.; Zummack, W.; Rabezzana, R.; Schwarz, H. *Angew. Chem., Int. Ed.* **1999**, *38*, 332–335.

(21) (a) Kobayashi, K.; Nagase, S. *Organometallics* **1997**, *16*, 2489–2491. (b) Nagase, S.; Kobayashi, K.; Takagi, N. *J. Organomet. Chem.* **2000**, *611*, 264–271.

(22) (a) Takagi, N.; Nagase, S. *Chem. Lett.* **2001**, 966–967. (b) Kobayashi, K.; Takagi, N.; Nagase, S. *Organometallics* **2001**, *20*, 234–236.

(23) Sekiguchi, A.; Kinjo, R.; Ichinohe, M. *Science* **2004**, *305*, 1755–1757.

(24) Sekiguchi, A.; Ichinohe, M.; Kinjo, R. *Bull. Chem. Soc. Jpn.* **2006**, *79*, 825–832.
(25) Fink, M. J.; Michalczyk, M. J.; Haller, K. J.; West, R.; Michl, J. *Organometallics* **1984**, *3*, 793–800.
(26) Power, P. P. *J. Chem. Soc., Dalton Trans.* **1998**, 2939–2951.
(27) Weidenbruch, M. *Eur. J. Inorg. Chem.* **1999**, 373–381.
(28) Bibal, C.; Mazieres, S.; Gornitzka, H.; Couret, C. *Angew. Chem., Int. Ed.* **2001**, *40*, 952–954.
(29) (a) (2,6-$Tip_2$-$C_6H_3$)PbPb($C_6H_3$-2,6-$Tip_2$), Tip = 2,4,6-$i Pr_3C_6H_2$: Pu, L. H.; Twamley, B.; Power, P. P. *J. Am. Chem. Soc.* **2000**, *122*, 3524–3525. (b) (2,6-$Dipp_2$-$C_6H_3$)SnSn($C_6H_3$-2,6-$Dipp_2$), Dipp = 2,6-$i Pr_2C_6H_3$: Phillips, A. D.; Wright, R. J.; Olmstead, M. M.; Power, P. P. *J. Am. Chem. Soc.* **2002**, *124*, 5930–5931. (c) (2,6-$Dipp_2$-$C_6H_3$)GeGe($C_6H_3$-2,6-$Dipp_2$): Stender, M.; Phillips, A. D.; Wright, R. J.; Power, P. P. *Angew. Chem., Int. Ed.* **2002**, *41*, 1785–1787. (d) Fischer, R. C.; Pu, L. H.; Fettinger, J. C.; Brynda, M. A.; Power, P. P. *J. Am. Chem. Soc.* **2006**, *128*, 11366–11367. (e) Fischer, R. C.; Power, P. P. *Chem. Rev.* **2010**, *110*, 3877–3923.
(30) For theoretical investigations of REER (E = Si−Pb) triple bonds: (a) Karni, M.; Apeloig, Y. *Chem. Isr.* **2005**, *19*, 22. (b) Karni, M.; Apeloig, Y.; Kapp, J.; Schleyer, P. v. R. In *The Chemistry of Organic Silicon Compounds*; Rappoport, Z., Apeloig, Y., Eds.; John Wiley & Sons: Chichester, U. K., 2001; Vol. 3, Chapter 1, pp 1−163. (c) Ganzer, I.; Hartmann, M.; Frenking, G. In *The Chemistry of Organic germanium, tin and lead Compounds*; Rappoport, Z., Ed.; John Wiley & Sons: Chichester, U. K., 2002; Vol. 2, Chapter 3, pp 169−282.
(31) For experimental studies of REER (E = Ge−Pb) triple bonds: (a) Power, P. P. *Chem. Comm* **2003**, 2091–2101 and references cited therein. (b) Weidenbruch, M. *Angew. Chem., Int. Ed.* **2003**, *42*, 2222–2224. (c) Weidenbruch, M. *Angew. Chem., Int. Ed.* **2005**, *44*, 514–516. (d) Sugiyama, Y.; Sasamori, T.; Hosoi, Y.; Furukawa, Y.; Takagi, N.; Nagase, S.; Tokitoh, N. *J. Am. Chem. Soc.* **2006**, *128*, 1023–1031.
(32) For discussions of the nature of the E−E bond in REER (M = Si, Ge, Sn), see: (a) Takagi, N.; Nagase, S. *Organometallics* **2001**, *20*, 5498–5500. (b) Lein, M.; Krapp, A.; Frenking, G. *J. Am. Chem. Soc.* **2005**, *127*, 6290–6299. (c) Jung, Y.; Brynda, M.; Power, P. P.; Head-Gordon, M. *J. Am. Chem. Soc.* **2006**, *128*, 7185–7192. (d) Grützmacher, H.; Fässler, T. F. *Chem.—Eur. J.* **2000**, *6*, 2317–2325. (e) Grunenberg, J. *Angew. Chem., Int. Ed.* **2001**, *40*, 4027–4029. (f) Malcolm, N. O. J.; Gillespie, R. J.; Popelier, P. L. A. *J. Chem. Soc., Dalton Trans.* **2002**, 3333–3341. (g) Chesnut, D. B. *Heteroatom Chem.* **2002**, *13*, 53–62. (h) Sugiyama, Y.; Sasamori, T.; Hosoi, Y.; Furukawa, Y.; Takagi, N.; Nagase, S.; Tokitoh, N. *J. Am. Chem. Soc.* **2006**, *128*, 1023–1031. (j) Bridgeman, A. J.; Ireland, L. R. *Polyhedron* **2001**, *20*, 2841–2851.
(33) (a) Pignedoli, C. A.; Curioni, A.; Andreoni, W. *ChemPhysChem* **2005**, *6*, 1795–1799. (b) Frenking, G.; Krapp, A.; Nagase, S.; Takagi, N.; Sekiguchi, A. *ChemPhysChem* **2006**, *7*, 799–800. (c) Pignedoli, C. A.; Curioni, A.; Andreoni, W. *ChemPhysChem* **2006**, *7*, 801–802.
(34) (a) Landis, C. R.; Weinhold, F. *J. Am. Chem. Soc.* **2006**, *128*, 7335–7345. (b) Weinhold, F.; Landis, C. R. *Science* **2007**, *316*, 61–63.
(35) Kravchenko, V.; Kinjo, R.; Sekiguchi, A.; Ichinohe, M.; West, R.; Balazs, T. S.; Schmidt, A.; Karni, M.; Apeloig, Y. *J. Am. Chem. Soc.* **2006**, *128*, 14472–14473.
(36) Schreiner, P.; Reisenauer, H. P.; Romanski, J.; Mloston, G. *Angew. Chem., Int. Ed.* **2009**, *48*, 8133–8136.
(37) Danovich, D.; Ogliaro, F.; Karni, M.; Apeloig, Y.; Cooper, D. L.; Shaik, S. *Angew. Chem., Int. Ed.* **2001**, *40*, 4023–4027; *Corrigenda. Angew. Chem., Int. Ed.* **2004**, *43*, 141–143.
(38) (a) Galbraith, J. M.; Blank, E.; Shaik, S.; Hiberty, P. C. *Chem.—Eur. J.* **2000**, *6*, 2425–2434. (b) Shaik, S.; Shurki, A.; Danovich, D.; Hiberty, P. C. *Chem. Rev.* **2001**, *101*, 1501–1539.
(39) (a) Shaik, S.; Maitre, P.; Sini, G.; Hiberty, P. C. *J. Am. Chem. Soc.* **1992**, *114*, 7861–7866. (b) Shaik, S.; Danovich, D.; Silvi, B.; Lauvergnat, D. L.; Hiberty, P. C. *Chem.—Eur. J.* **2005**, *11*, 6358–6371. (c) Shaik, S.; Danovich, D.; Wu, W.; Hiberty, P. C. *Nature Chem.* **2009**, *1*, 443–449. (d) Zhang, L. X.; Ying, F. M.; Wu, W.; Hiberty, P. C.; Shaik, S. *Chem.—Eur. J.* **2009**, *15*, 2979–2989. (e) Hiberty, P. C.; Ramozzi, R.; Song, L. C.; Wu, W.; Shaik, S. *Faraday Discuss.* **2007**, *135*, 261–272. (f) Rzepa, H. S. *Nature Chem.* **2010**, *2*, 390–393.
(40) (a) For an early model of bonding in bent double bonds, see: Trinquier, G.; Malrieu, J. P. *J. Am. Chem. Soc.* **1987**, *109*, 5303–5315. Trinquier, G.; Malrieu, J. P. *J. Phys. Chem.* **1990**, *94*, 6184–6196. (b) Trinquier, G.; Malrieu, J.-P. *J. Am. Chem. Soc.* **1989**, *111*, 5916–5921.(c) For an early consideration of the effect of fragment states on the bond dissociation energies of double bonds, see: Carter, E. A.; Goddard, W. A. *J. Phys. Chem.* **1986**, *90*, 998–1001.
(41) (a) Shaik, S.; Hiberty, P. C. *A Chemist's Guide to Valence Bond Theory*; Wiley-Interscience: Hobboken, NJ, 2008, pp 26−41. (b) Shaik, S.; Hiberty, P. C. *Rev. Comput. Chem.* **2004**, *20*, 1–100.
(42) (a) Hiberty, P. C.; Danovich, D.; Shurki, A.; Shaik, S. *J. Am. Chem. Soc.* **1995**, *117*, 7760–7768. (b) Jug, K.; Hiberty, P. C.; Shaik, S. *Chem. Rev.* **2001**, *101*, 1477–1500. (c) Wu, W.; Gu, J. J.; Song, J. S.; Shaik, S.; Hiberty, P. C. *Angew. Chem., Int. Ed.* **2009**, *48*, 1407–1410. (d) Shaik, S.; Chen, Z. H.; Wu, W.; Stanger, A.; Danovich, D.; Hiberty, P. C. *ChemPhysChem* **2009**, *10*, 2658–2669.
(43) (a) Kutzelnigg, W. The physical origin of the chemical bond. In *Theoretical Models of Chemical Bonding*; Springer: New York, 1990, part 2, pp 1−44. (b) Ruedenberg, K. *Rev. Mod. Phys.* **1962**, *34*, 326–376. (c) Feinberg, M. J.; Ruedenberg, K. *J. Chem. Phys.* **1971**, *54*, 1495–1591. (d) The role of kinetic energy in chemical binding: Wilson, C. W.; Goddard, W. A. *Theor. Chim. Acta.* **1972**, *26*, 195–210. (e) Rozendaal, A.; Baerends, E. J. *Chem. Phys.* **1985**, *95*, 57–91. (f) Ruedenberg, K.; Schmidt, M. W. *J. Comput. Chem.* **2007**, *28*, 391–410. (g) Bickelhaupt, F. M.; Baerends, E. J. *Rev. Comput. Chem.* **2000**, *15*, 1–86.
(44) (a) Chirgwin, H. B.; Coulson, C. A. *Proc. R. Soc. London, Ser. A* **1950**, *201*, 196–209. (b) Gallup, G. A.; Norbeck, J. M. *Chem. Phys. Lett.* **1973**, *21*, 495–500.
(45) Frisch, M. J.; Trucks, G. W.; Schlegel, H. B.; Scuseria, G. E.; Robb, M. A.; Cheeseman, J. R.; Montgomery, J. A., Jr.; Vreven, T.; Kudin, K. N.; Burant, J. C.; Millam, J. M.; Iyengar, S. S.; Tomasi, J.; Barone, V.; Mennucci, B.; Cossi, M.; Scalmani, G.; Rega, N.; Petersson, G. A.; Nakatsuji, H.; Hada, M.; Ehara, M.; Toyota, K.; Fukuda, R.; Hasegawa, J.; Ishida, M.; Nakajima, T.; Honda, Y.; Kitao, O.; Nakai, H.; Klene, M.; Li, X.; Knox, J. E.; Hratchian, H. P.; Cross, J. B.; Bakken, V.; Adamo, C.; Jaramillo, J.; Gomperts, R.; Stratmann, R. E.; Yazyev, O.; Austin, A. J.; Cammi, R.; Pomelli, C.; Ochterski, J. W.; Ayala, P. Y.; Morokuma, K.; Voth, G. A.; Salvador, P.; Dannenberg, J. J.; Zakrzewski, V. G.; Dapprich, S.; Daniels, A. D.; Strain, M. C.; Farkas, O.; Malick, D. K.; Rabuck, A. D.; Raghavachari, K.; Foresman, J. B.; Ortiz, J. V.; Cui, Q.; Baboul, A. G.; Clifford, S.; Cioslowski, J.; Stefanov, B. B.; Liu, G.; Liashenko, A.; Piskorz, P.; Komaromi, I.; Martin, R. L.; Fox, D. J.; Keith, T.; Al-Laham, M. A.; Peng, C. Y.; Nanayakkara, A.; Challacombe, M.; Gill, P. M. W.; Johnson, B.; Chen, W.; Wong, M. W.; Gonzalez, C.; Pople, J. A. *Gaussian 03*, Revision E.01; Gaussian, Inc.: Wallingford, CT, 2004.
(46) Song, I.; Wu, W.; Mo, Y.; Zhang, Q. *XMVB-0.1*; Xiamen University: Xiamen, China, 2003.
(47) van Lenthe, J. H.; Balint-Kurti, G. G. *J. Chem. Phys.* **1983**, *78*, 5699–5713.
(48) (a) Hiberty, P. C.; Flament, J. P.; Noizet, E. *Chem. Phys. Lett.* **1992**, *189*, 259–265. (b) Hiberty, P. C.; Humbel, S.; Byrman, C. P.; Vanlenthe, J. H. *J. Chem. Phys.* **1994**, *101*, 5969–5976. (c) Hiberty, P. C.; Shaik, S. *Theor. Chem. Acc.* **2002**, *108*, 255–272.
(49) Pyykko, P.; Riedel, S.; Patzschke, M. *Chem.—Eur. J.* **2005**, *11*, 3511–3520.
(50) Sanderson, R. T. *Polar Covalence*; Academic Press, New York, 1983.
(51) Allred, A. L.; Rochow, E. G. *J. Inorg. Nucl. Chem.* **1958**, *5*, 264–268.
(52) Lauvergnat, D.; Hiberty, P. C. *THEOCHEM* **1995**, *338*, 283–291.
(53) Pauling, L. *The Nature of the Chemical Bond*, 3rd ed.; Cornell University Press: Ithaca, 1960; pp 80−83.
(54) Sugiyama, Y.; Sasmori, T.; Hosoi, Y.; Furukawa, Y.; Takagi, N.; Nagase, S.; Tokitoh, N. *J. Am. Chem. Soc.* **2006**, *128*, 1023–1031.